Journal of Molecular Spectroscopy 388 (2022) 111684

Contents lists available at ScienceDirect

Journal of Molecular Spectroscopy

journal homepage: www.elsevier.com/locate/yjmsp

The 130–360 GHz rotational spectrum of isocyanocyclobutane (C_4H_7NC) and cyanocyclobutane (C_4H_7CN)

Brian J. Esselman, Samuel M. Kougias, Madison D. Fellows, R. Claude Woods *, Robert J. McMahon *

Department of Chemistry, University of Wisconsin–Madison, Madison, WI 53706, USA

A B S T R A C T

The 130–360 GHz rotational spectrum of isocyanocyclobutane is reported herein for the first time. Over 2200 transitions were measured, assigned, and least-squares fit to a partial-octic distorted-rotor Hamiltonian with small deviation ($\sigma_{fit} < 50$ kHz) for the *equatorial* conformer. The *axial* conformer has so far remained elusive. For cyanocyclobutane, we measured the rotational spectra of both *equatorial* and *axial* conformers in the same frequency region to allow a direct comparison between the isomers. Transition frequencies for each conformational isomer of cyanocyclobutane were similarly fit to partial octic distorted-rotor Hamiltonians with small deviation. The experimental spectroscopic constants are in very good agreement with the predicted values (B3LYP) for all three species and with those reported in an earlier microwave study of cyanocyclobutane. Measurement of the relative transition intensities provides an updated energy difference of 0.69 (7) kcal/mol between the two conformers, with the equatorial conformation being the more stable one. Analysis of the *axial* conformation of cyanocyclobutane reveals coupling of its ground state to the vibrationally excited states of the *equatorial* conformation. Our observations of the vibrationally excited states of the *equatorial* conformer suggest that there are many Coriolis interactions between these states that were not described previously. Combined with literature values of nuclear quadrupole coupling constants, these spectroscopic constants and reported transition frequencies provide the basis for future astronomical searches for isocyanocyclobutane and cyanocyclobutane.

1. Introduction

Nitriles (R–CN) are prominently represented in the list of more than 260 molecules detected in extraterrestrial environments [1,2] due to their stability, relative abundance, and intrinsically large dipole moments. In many instances, the corresponding isonitriles (R–NC) have also been detected, *e.g.*, R = H [3,4], R = CH_3 [5,6], and R = HCC [7]. These molecules reflect the full range of unsaturation (hydrogenation) available to organic species – from maximally unsaturated carbon chains [7–14] to intermediate levels of unsaturation (aromatic nitriles [15,16] and cyanocyclopentadienes [17,18]) to fully saturated frameworks (propyl [19] and isopropyl cyanide [20]). All of these molecular detections provide evidence for a rich chemistry involving organic nitriles in extraterrestrial environments. While none of the previously detected species includes a four-membered organic ring, the detections of propyl and isopropyl cyanide raise the possibility of detecting species such as cyanocyclobutene [21], cyanocyclobutane, and isocyanocyclobutane. Astronomical detection of these species is dependent on accurate experimental and predicted transition frequencies across the spectral range of available radiotelescopes.

Cyanocyclobutane and isocyanocyclobutane (Fig. 1) exist as equilibrium mixtures of two C_s conformational isomers, each with *a*- and *c*-type rotational transitions. The lower energy isomer, cyanocyclobutane (*c*-C_4H_7-CN) has been well-studied spectroscopically. Its vibrational spectra (infrared and Raman) have been reported and assigned in the solid, liquid, gas, and matrix phases [22–24] for both the *equatorial* and *axial* conformational isomers. In contemporaneous microwave spectroscopy works from 1973, two groups reported the rotational spectra of *equatorial* cyanocyclobutane [25,26]. Fong *et al.* reported the spectrum from 13 to 32 GHz and determined the ^{14}N nuclear quadrupole coupling constants, dipole moment components, and spectroscopic constants for the ground vibrational state and four vibrationally excited states of the ring-puckering (ν_{20}, A′) and out-of-plane vibrational modes (ν_{33}, A″) [25]. Durig *et al.* measured the spectrum from 26 to 40 GHz and reported dipole moment components and spectroscopic constants for the ground vibrational state and five vibrationally excited states of the ring-puckering (ν_{20}) and out-of-plane nitrile bending (ν_{33}) vibrational modes [26]. Caminati *et al.* reinvestigated the spectrum of cyanocyclobutane and improved the set of spectroscopic constants by determining the quartic centrifugal distortion constants [27]. They also observed the *axial* conformer for the first time [27], after a combined *ab initio* study and electron diffraction study of 1,1-dicyanocyclobutane suggested the

* Corresponding authors.
E-mail addresses: rcwoods@wisc.edu (R.C. Woods), robert.mcmahon@wisc.edu (R.J. McMahon).

https://doi.org/10.1016/j.jms.2022.111684
Received 20 May 2022; Received in revised form 20 June 2022; Accepted 25 July 2022
Available online 29 July 2022

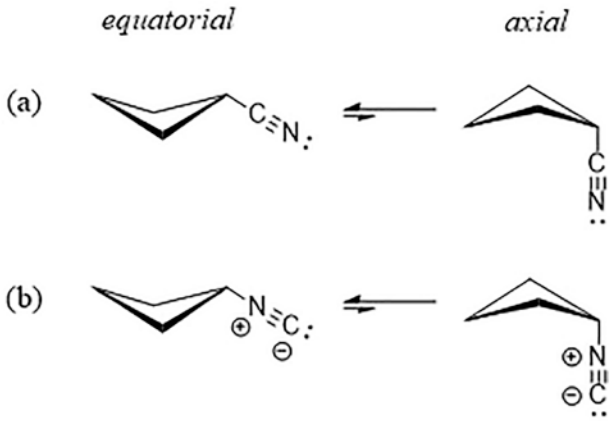

Fig. 1. (a) *Equatorial* and *axial* conformers of cyanocyclobutane. (b) *Equatorial* and *axial* conformers of isocyanocyclobutane.

existence of distinct *axial* and *equatorial* substituent positions [28]. In a related work, Caminati *et al*. analyzed the ring-puckering potential and reported spectroscopic constants for an additional five vibrationally excited states of *equatorial* cyanocyclobutane and five vibrationally excited states of *axial* cyanocyclobutane, including the out-of-plane nitrile-bending vibrational mode (ν_{19}, A′) [29]. Importantly, the latter work corrected the previous assignments of the vibrationally excited state spectra of the *equatorial* conformers. The data sets in these studies contained limited numbers of low-*J* transitions (<60 transitions) with frequencies less than 40 GHz. Thus, it is not surprising that no Coriolis coupling was reported between the vibrationally excited states despite several small energy spacings between states.

Like other cycloalkanes, the non-planarity of the cyclobutane ring gives rise to two non-equivalent conformational isomers of mono-substituted cyclobutane derivatives in which the substituent can occupy an *equatorial* or an *axial* position [22,29–32], (Fig. 1). Experimentally, the enthalpy difference between the *axial* and *equatorial* conformations of cyanocyclobutane has been reported to be 0.73 (14) kcal/mol, favoring the *equatorial* conformation with a barrier to conformational interconversion of less than 2.3 kcal/mol [22,27,29]. The potential energy surfaces of cyano- and isocyano cyclobutane are similar to those of chloro- or bromocyclobutane, whose rings are likewise substituted with σ electron-withdrawing substituents with a low steric profile [33]. Isomerization of isocyanocyclobutane (R–NC) to the lower energy nitrile isomer (R–CN occurs thermally at 200 °C. Although the enthalpies of formation and isomerization have not been measured directly for R = cyclobutyl, such isomerizations have been well studied and are remarkably similar, regardless of the R group [34]. As a result, the isocyano isomer is expected to be ~ 21 kcal/mol higher in energy than the cyano isomer, with an isomerization energy barrier of ~ 38 kcal/mol [35,36]. Thus, the rate of gas-phase isomerization at room temperature is negligible, and each of these cyclobutane derivatives can be studied independently.

Compared to cyanocyclobutane, relatively little is known about isocyanocyclobutane [37,38]. Isocyanocyclobutane has been synthesized previously [37,39,40], though its characterization is limited. It was recently used to generate a substituted tetrazole *via* an Ugi-azide, three-component reaction [41]. The present work describes the synthesis, purification, and characterization of isocyanocyclobutane and the rotational spectroscopy of both isocyano- and cyanocyclobutane.

2. Computational methods

Electronic structure calculations were carried out with Gaussian 16 [42] using the WebMO interface [43] to obtain theoretical spectroscopic constants. Optimized geometries at the B3LYP/6-311+(2d,p) level were obtained using "verytight" convergence criteria and an "ultrafine" integration grid, and subsequent anharmonic vibrational frequency calculations were carried out. All computational output files can be found in the supplemental material.

3. Experimental methods

3.1. Synthesis

We are not aware of commercial sources of isocyanocyclobutane. Like many other isonitriles, it can be readily prepared by dehydration of the corresponding formamide [37,44]. The requisite formamide, *N*-cyclobutylformamide, is generated *via* nucleophilic acyl substitution with excess ethyl formate in a 97 % yield (Scheme 1). Subsequently, *N*-cyclobutylformamide is dehydrated using a slight excess of *p*-toluenesulfonyl chloride (TsCl) in quinoline. Isocyanocyclobutane is then distilled into a liquid nitrogen-cooled receiving flask and purified *via* trap-to-trap vapor distillation twice, to remove any residual quinoline. Isocyanocyclobutane was obtained in a 40 % yield, characterized, and its rotational spectrum obtained. Characteristically of isonitriles, the odor of this compound is both intense and foul, and all contaminated glassware should be soaked in a bleach solution. A detailed experimental procedure and characterization is provided in Section 6 (*vide infra*).

3.2. Spectroscopy

Using a millimeter-wave spectrometer that has been previously described [45,46], the rotational spectra of both cyclobutane derivatives were collected from 130 to 230 and from 235 to 360 GHz, in a continuous flow at room temperature, with a sample pressure of 3 mTorr. A commercial sample of cyanocyclobutane was used without further purification, while isocyanocyclobutane was synthesized as described. The separate spectral segments were combined into a single broadband spectrum using Kisiel's Assignment and Analysis of Broadband Spectra (AABS) software [47,48]. The complete spectrum from 130 to 360 GHz was obtained automatically over approximately six days using the following experimental parameters: 0.6 MHz/*sec* sweep rate, 10 ms time constant, and 50 kHz AM and 500 kHz FM modulation in a tone burst design. Pickett's SPFIT/SPCAT [49] were used for least-squares fits and spectral predictions [47,48], along with Kisiel's PIFORM, PLANM, and AC programs for analysis [47,48]. A uniform frequency measurement uncertainty of 0.050 MHz was assumed for all measurements.

4. Results

4.1. Cyanocyclobutane

Equatorial cyanocyclobutane (Fig. 2a) is a highly prolate ($\kappa = -0.927$), asymmetric top with dipole moment components along its *a*- and *c*-principal axes ($\mu_a = 4.04 \pm 0.09$ D, $\mu_c = 0.92 \pm 0.03$ D [26]) resulting in strong *a*- and much weaker *c*-type rotational transitions. The *axial*

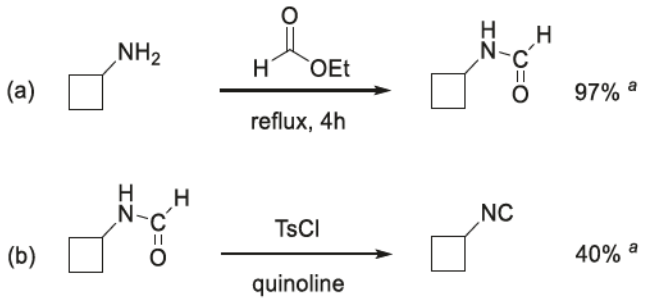

Scheme 1. Syntheses of *N*-cyclobutylformamide and isocyanocyclobutane.

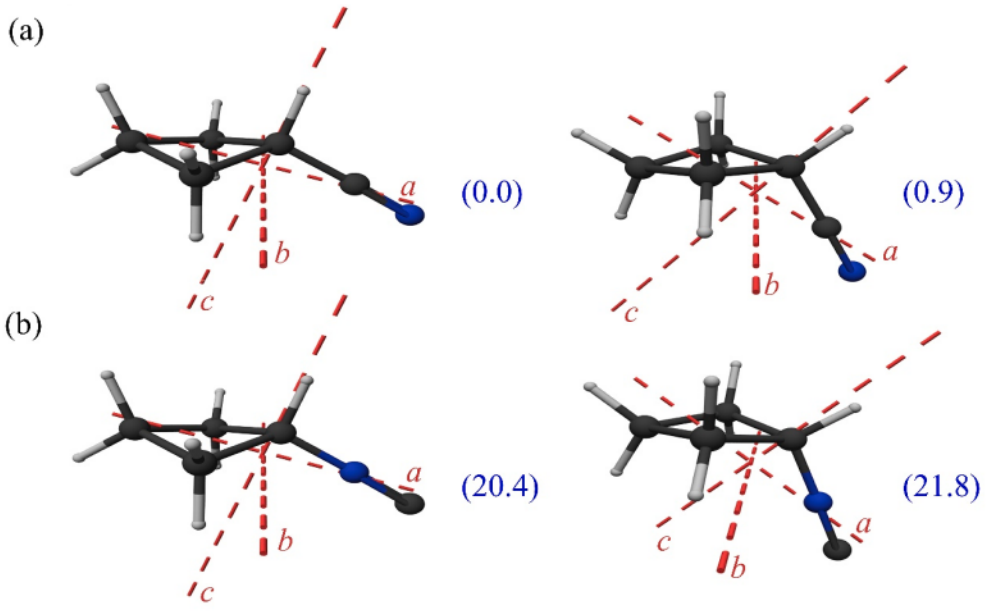

Fig. 2. (a) *Equatorial* ($\mu_a = 4.04 \pm 0.09$ D, $\mu_c = 0.92 \pm 0.03$ D [26]) and *axial* ($\mu_a = 3.81 \pm 0.03$ D, $\mu_c = 1.34 \pm 0.03$ D [27]) conformers of cyanocyclobutane. (b) *Equatorial* ($\mu_a = 4.01$ D, $\mu_c = 0.92$ D, B3LYP) and *axial* ($\mu_a = 3.90$ D, $\mu_c = 1.26$ D, B3LYP) conformers of isocyanocyclobutane. The computed relative energies in kcal/mol are presented in parenthesis, including zero-point vibrational energy correction.

conformer (Fig. 2a) is also a highly prolate ($\kappa = -0.931$) asymmetric top with a dipole along its *a*- and *c*-principal axes (($\mu_a = 3.81 \pm 0.03$ D, $\mu_c = 1.34 \pm 0.03$ D [27]). Caminati *et al.* determined an energy difference of 0.73 ± 0.14 kcal/mol [27], favoring the *equatorial* conformation [27]. The resulting spectrum from 130 to 360 GHz of cyanocyclobutane is dominated by $^{a}R_{0,1}$ transitions from the *equatorial* conformation, with weaker Q-branch transitions. Additionally, there are many R- and Q-branch transitions from its vibrationally excited states and its *axial* conformational isomer. Previously reported spectroscopic constants were combined with computed sextic centrifugal distortion constants to guide our initial search and assignment. Fig. 3 shows the rotational spectrum from 191.5 to 199.2 GHz, with the typical prolate-band structure of a highly prolate asymmetric top created by transitions of the same J'. The $J' = 43$ and $J' = 44$ bands of *equatorial* cyanocyclobutane (Fig. 3) are created by degenerate K_a^+ and K_a^- transitions (those where $K_a + K_c = J$ and $K_a + K_c = J + 1$, respectively) that progress to lower frequency and, at moderate K_a, turnaround and then progress toward higher frequency. Similar, but less intense bands ($J' = 37$ and $J' = 38$) are visible for *axial* cyanocyclobutane. The prominence of these features, combined with the excellent initial spectroscopic predictions for both conformational isomers, made the preliminary assignments and least-squares fitting relatively straightforward.

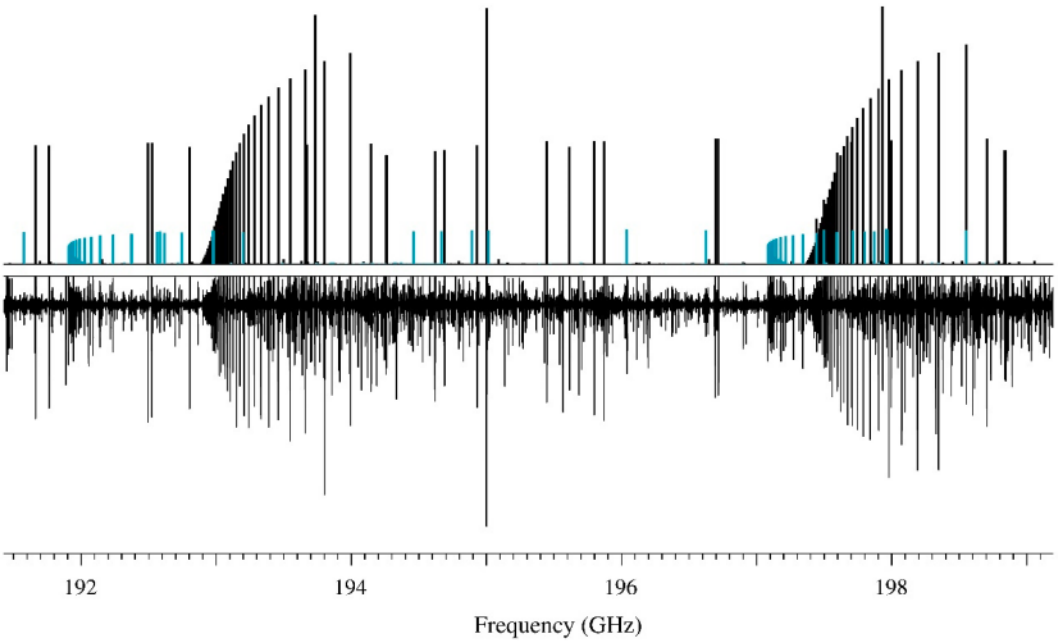

Fig. 3. Predicted (top) and experimental (bottom) rotational spectra of cyanocyclobutane from 191.5 to 199.2 GHz. Ground-state *equatorial* cyanocyclobutane transitions for the $J' = 43$ and $J' = 44$ bands appear in black. Ground-state *axial* cyanocyclobutane transitions for the $J' = 37$ and $J' = 38$ bands appear in cyan. Unassigned transitions are predominantly attributable to vibrationally excited states of *equatorial* cyanocyclobutane.

4.2. Equatorial cyanocyclobutane

Over 3100 R- and Q-branch transitions have been measured, assigned, and least-squares fit for *equatorial* cyanocyclobutane to both an A- and S-reduced, partial-octic centrifugally distorted Hamiltonian models in the I^r representation. Across the frequency range of this study, nuclear quadrupole splitting from the nitrogen nucleus was not resolved. Thus, these terms were not included in the Hamiltonian. The broad range of J' (2 to 86) and K_a' (0 to 54) values shown in the data set distribution plot in Fig. 4, necessitated the inclusion of a complete set of sextic centrifugal distortion constants and two octic centrifugal distortion terms (L_{JK} and L_{KKJ}) in both the S- and A-reductions ($\sigma_{fit} = 0.032$ MHz). While the data set is dominated by $^aR_{0,1}$ transitions, approximately 10 % of the R-branch transitions included in the data set, and all of the Q-branch transitions, are *c*-type transitions. Previously reported microwave transitions from Caminati *et al.* [27] were included in the data set and are represented in Fig. 4 by blue symbols. The resulting spectroscopic constants are presented in Table 1, and the least-squares fitting output files can be found in the supplemental material. Computed spectroscopic constants, where available, are presented alongside the experimental values in Table 1 for comparison. As expected, the computed A_0, B_0, and C_0 terms are within 1.6, 0.4, and 0.5 %, respectively, of their experimental values in both reductions. The computed quartic centrifugal distortion terms are in generally good agreement – within 7 % of their experimental values, except for D_{JK} and Δ_{JK}. These computed values D_{JK} and Δ_{JK} deviate by 25 and 28 % from their experimental values, respectively. The experimental Δ_{JK} value (0.776529 (84) MHz) determined in this work is in closer agreement with the value from the partial-quartic least-squares fit presented by Caminati *et al.* (0.96 (1) MHz) [29]. Given the extensive data sets, low σ_{fit} value, and the underestimate of the corresponding constant in each reduction, we attribute the discrepancy almost entirely to the computational model and not to the experimental least-squares fit. All of the computed sextic centrifugal distortion constants are in reasonable agreement (within 10 %) of the experimental values, except h_1, h_2, Φ_{JK}, and ϕ_{JK}. Without a data set that supports determination of a complete set of octic distortion constants, it is more challenging to ascertain the source of the deviation in these constants. The discrepancy may be an extension of the issue with the computed values of D_{JK} and Δ_{JK} or could be due to a truncation of the model and the incorporation of missing effects of the octic terms into the sextic terms during the least-squares fitting. With all experimental constants well-determined and of the expected sign and magnitude, we are confident in their physical meaning and that the ground state of the *equatorial* conformation is generally free of Coriolis coupling with its vibrationally excited states across the frequency range of our measurements.

Even though it was not noted in previous studies, our preliminary analysis of the vibrationally excited states of *equatorial* cyclobutane in the 130 to 360 GHz range revealed that there are clearly Coriolis interactions between ν_{20} (142 cm^{-1} [24]) and ν_{33} (192 cm^{-1} [24]) preventing either state from being adequately treated by a single-state Hamiltonian model. Given the close proximity of the next fundamental ν_{19} (262 cm^{-1} [24]) and the first set of overtones and combination $2\nu_{20}$ (~284 cm^{-1}), $\nu_{20} + \nu_{33}$ (334 cm^{-1}), and $2\nu_{33}$ (384 cm^{-1}), it is not yet clear whether ν_{20} and ν_{33} could be treated as an isolated dyad or must be analyzed as part of a larger polyad. Analysis of this complex system of vibrationally excited states is beyond the scope of the current work.

4.3. Axial cyanocyclobutane

As shown in Fig. 3 (cyan), the rotational spectrum of *axial* cyanocyclobutane ($\mu_a = 3.81 \pm 0.03$ D, $\mu_c = 1.34 \pm 0.03$ D, $\kappa = -0.931$ [27]) is readily identifiable by the distinct prolate-type bands of lesser intensity than the *equatorial* conformer. With a larger value of C_0, these bands appear to migrate across the spectrum with respect to the ground state and vibrationally excited states of the *equatorial* conformer. The initial prediction was based upon the previous reported spectroscopic constants [29] combined with computed centrifugal distortion constants. This prediction was sufficient to assign the transitions of the *axial* conformation in a straightforward manner. The least-squares fitting of *axial* cyanocyclobutane, however, is not as straightforward, as its transitions are *not* well-modeled by a single-state Hamiltonian. This is not surprising given the close energy spacing of the *axial* ground state (~240 cm^{-1}) and $2\nu_{20}$ (~284 cm^{-1}) of the *equatorial* conformer. The close energy spacing, ring-puckering potential function, and wave function for the lowest several ring-puckering vibrational states of both conformers were first described by Caminati *et al.* and are well-illustrated in Fig. 2 of that work [29] where $2\nu_{20}$ is vibrational state 2 (also labeled v(0, 2) by Durig *et al.* [26]). The spectroscopic constants presented in Table 2 are from an effective least-squares fit that is

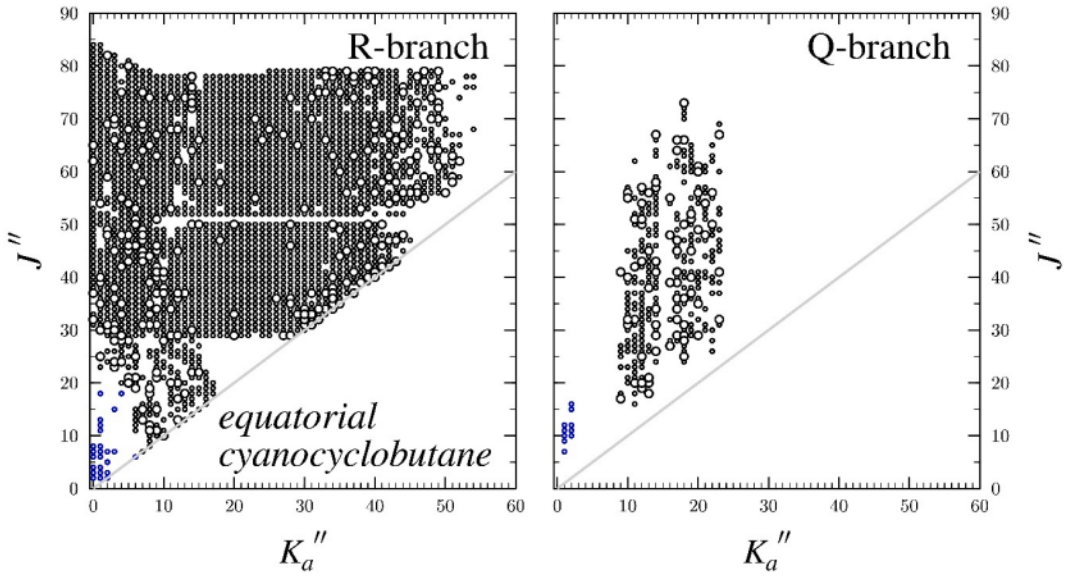

Fig. 4. Data distribution plots for the least-squares fit of spectroscopic data for the vibrational ground state of *equatorial* cyanocyclobutane. The size of the symbol is proportional to the value of $|(f_{obs.} - f_{calc.})/\delta f|$, where δf is the frequency measurement uncertainty, and all values are smaller than 3. Transitions from Caminati *et al.* [27] are in blue.

Table 1
Spectroscopic constants for the ground vibrational state of *equatorial* cyanocyclobutane (S- and A-reduced Hamiltonian, I^r representation).

	S Reduction, I^r representation			A Reduction, I^r representation	
	Experimental	B3LYP [a]		Experimental	B3LYP [a]
A_0 (MHz)	9761.90298 (22)	9604.	A_0 (MHz)	9761.90288 (22)	9604.
B_0 (MHz)	2383.395088 (44)	2375.	B_0 (MHz)	2383.398238 (44)	2375.
C_0 (MHz)	2105.124237 (47)	2094.	C_0 (MHz)	2105.121126 (48)	2094.
D_J (kHz)	0.3575750 (96)	0.349	Δ_J (kHz)	0.372006 (12)	0.362
D_{JK} (kHz)	0.863158 (66)	0.643	Δ_{JK} (kHz)	0.776529 (84)	0.562
D_K (kHz)	14.41358 (79)	15.4	Δ_K (kHz)	14.48570 (79)	15.5
d_1 (kHz)	−0.0152819 (70)	−0.0152	δ_J (kHz)	0.0152839 (70)	0.0152
d_2 (kHz)	−0.0072134 (39)	−0.00680	δ_K (kHz)	1.56035 (87)	1.45
H_J (Hz)	0.00045004 (82)	0.000437	Φ_J (Hz)	0.0004624 (13)	0.000451
H_{JK} (Hz)	−0.0045818 (83)	−0.00492	Φ_{JK} (Hz)	−0.00193 (18)	−0.00259
H_{KJ} (Hz)	0.063659 (53)	0.0628	Φ_{KJ} (Hz)	0.05457 (62)	0.0549
H_K (Hz)	−0.19705 (83)	−0.207	Φ_K (Hz)	−0.19079 (94)	−0.202
h_1 (Hz)	−0.00001113 (74)	−0.0000134	ϕ_J (Hz)	−0.00000792 (78)	−0.0000106
h_2 (Hz)	0.00000580 (54)	0.00000678	ϕ_{JK} (Hz)	0.00116 (11)	0.00122
h_3 (Hz)	0.00000301 (22)	0.00000282	ϕ_K (Hz)	0.0871 (66)	0.0767
L_J (mHz)	[0.]		L_J (μHz)	[0.]	
L_{JJK} (mHz)	[0.]		L_{JJK} (μHz)	[0.]	
L_{JK} (mHz)	−0.0005260 (42)		L_{JK} (μHz)	−0.0005922 (57)	
L_{KKJ} (mHz)	0.002274 (16)		L_{KKJ} (μHz)	0.002479 (21)	
L_K (mHz)	[0.]		L_K (μHz)	[0.]	
Δ_i (uÅ^2)[b,c]	−23.741314 (7)		Δ_i (uÅ^2)[b,c]	−23.740679 (7)	
P_{bb} (uÅ^2)[c,d]	39.899885 (3)		P_{bb} (uÅ^2)[c,d]	39.900203 (3)	
N_{lines} [e]	3158		N_{lines} [e]	3158	
σ_{fit} (MHz)	0.032		σ_{fit} (MHz)	0.032	

[a] Evaluated with the 6–311+G(2d,p) basis set. The computational output files label the representation as II^l, though we are confident that those constants are I^l which have been converted to I^r.
[b] Inertial defect, $\Delta_i = I_c - I_a - I_b$.
[c] Calculated using PLANM from the B_0 constants.
[d] Second moment, $P_{bb} = (I_c + I_a - I_b)/2$.
[e] Number of fitted transition frequencies.

Table 2
Effective spectroscopic constants for the ground vibrational state of *axial* cyanocyclobutane (S- and A-reduced Hamiltonian, I^r representation).

	S Reduction, I^r representation			A Reduction, I^r representation	
	Experimental	B3LYP [a]		Experimental	B3LYP [a]
A_0 (MHz)	7591.981 (25)	7834.2	A_0 (MHz)	7592.078 (22)	7834.2
B_0 (MHz)	2681.97940 (47)	2590.3	B_0 (MHz)	2681.98130 (48)	2590.3
C_0 (MHz)	2505.93868 (48)	2381.0	C_0 (MHz)	2505.93695 (50)	2381.0
D_J (kHz)	1.332174 (35)	1.37	Δ_J (kHz)	1.339432 (38)	1.39
D_{JK} (kHz)	−3.21013 (12)	−4.72	Δ_{JK} (kHz)	−3.25344 (15)	−4.80
D_K (kHz)	12.34 (16)	18.1	Δ_K (kHz)	12.29 (16)	18.2
d_1 (kHz)	0.128959 (74)	0.150	δ_J (kHz)	−0.129066 (75)	−0.150
d_2 (kHz)	−0.003906 (39)	−0.00635	δ_K (kHz)	0.8223 (20)	1.34
H_J (Hz)	−0.0000667 (37)	−0.00191	Φ_J (Hz)	−0.0002301 (38)	−0.00209
H_{JK} (Hz)	0.011221 (13)	0.0304	Φ_{JK} (Hz)	0.011729 (13)	0.0310
H_{KJ} (Hz)	−0.042825 (40)	−0.149	Φ_{KJ} (Hz)	−0.041946 (41)	−0.148
H_K (Hz)	[0.463]	0.463	Φ_K (Hz)	[0.462]	0.462
h_1 (Hz)	0.0002759 (80)	0.000767	ϕ_J (Hz)	0.0002650 (81)	0.000767
h_2 (Hz)	−0.0000405 (54)	−0.0000909	ϕ_{JK} (Hz)	[−0.0163]	−0.0163
h_3 (Hz)	[−0.000000544]	−0.000000544	ϕ_K (Hz)	[−0.0246]	−0.0246
Δ_i (uÅ^2)[b,c]	−53.33002 (23)		Δ_i (uÅ^2) [b,c]	−53.32890 (20)	
P_{bb} (uÅ^2)[c,d]	39.902465 (3)		P_{bb} (uÅ^2) [c,d]	39.902176 (3)	
N_{lines} [e]	987		N_{lines} [e]	987	
σ_{fit} (MHz)	0.040		σ_{fit} (MHz)	0.040	

[a] Evaluated with the 6–311+G(2d,p) basis set. The computational output files label the representation as II^l, though we are confident that those constants are I^l which have been converted to I^r.
[b] Inertial defect, $\Delta_i = I_c - I_a - I_b$.
[c] Calculated using PLANM from the B_0 constants.
[d] Second moment, $P_{bb} = (I_c + I_a - I_b)/2$.
[e] Number of fitted transition frequencies.

predictive for many of the most intense spectroscopic features of the spectrum of the *axial* conformer, but for which noticeably perturbed transition frequencies were removed from the data set. As with the *equatorial* conformation, previously reported microwave transitions from Caminati *et al.* [27] were included in the data set and are represented in Fig. 5 by blue symbols. The data set distribution plot (Fig. 5) shows curving gaps created by perturbed transitions that could not be included in the least-squares fit. Despite the removal of many hundreds of transitions, it is not possible to obtain a single-state fit of *axial* cyanocyclobutane with centrifugal distortion constants that match the sign and magnitude of the computed constants. In order to model these transitions adequately, a multi-state Hamiltonian model would be

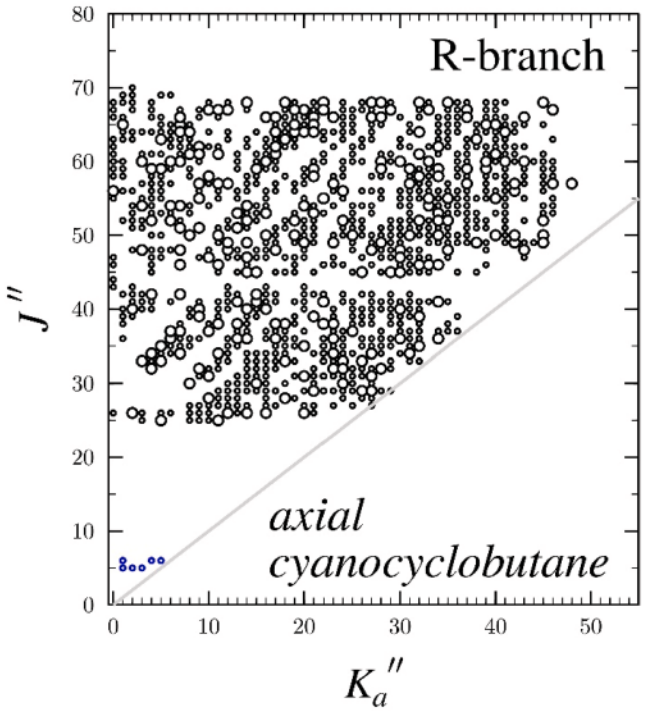

Fig. 5. Data distribution plot for the least-squares fit of spectroscopic data for the vibrational ground state of *axial* cyanocyclobutane. The size of the symbol is proportional to the value of $|(f_{obs.} - f_{calc.})/\delta f|$, where δf is the frequency measurement uncertainty. The curving gaps in the data distribution plot are suggestive of strongly perturbed transitions and untreated Coriolis coupling. Transitions from Caminati *et al.* [27] are in blue.

necessary, including the *c*-axis Coriolis interactions of the *axial* ground state (A′), $2\nu_{20}$ (A′) of the *equatorial* conformer, and ν_{19} (A′) of the *equatorial* conformer. Analysis of these interactions is beyond the scope of the current work.

4.4. Equatorial isocyanocyclobutane

Like the cyano isomer, *equatorial* isocyanocyclobutane (Fig. 2b) is a highly prolate ($\kappa =$ − 0.916), asymmetric top with dipole moment components along its *a*- and *c*-principal axes ($\mu_a = 4.12$ D, $\mu_c = 0.92$ D, B3LYP). No previous rotational constants have been reported for this molecule, so the initial predictions of its rotational spectrum were based upon computed rotational and centrifugal distortion constants. Using this method, over 2200 transitions of the *equatorial* conformer of isocyanocyclobutane were readily measured, assigned, and least-squares fit to a sextic A- and S-reduced, partial-octic centrifugally distorted Hamiltonian models in the I^r representation. These transitions span a comparable *J* and K_a range (Fig. 6) to those of *equatorial* cyanocyclobutane (Fig. 4). The rotational spectrum of isocyanocyclobutane (Fig. 7) displays a very similar structure and appearance to that of cyanocyclobutane (Fig. 3). This result is to be expected because the structural differences between the isomers (isocyano vs cyano group) lead to relatively small differences in the rotational and centrifugal distortion constants. Relative to *equatorial* cyanocyclobutane (Table 1), the spectroscopic constants of *equatorial* isocyanocyclobutane (Table 3) change by only a moderate amount. With the CN-moiety lying quite close to the *a*-principal axis, the change in A_0 is quite small (0.63 %). The changes in B_0 and C_0 are larger, reflecting the exchange of the carbon and nitrogen masses on their respective moments of inertia, but they still change by only 6.7 and 5.7 %, respectively. The changes in the centrifugal distortion constants are larger, but nevertheless the constants are generally consistent between the two isomers. Due to the decreased number of transitions available in the spectrum of isocyanocyclobutane – possibly due a lower partial pressure of isocyanocyclobutane in the gas sample, overlapping signals with impurities in the synthesized sample, or vibrationally excited states across the experimental spectrum – two of the off-diagonal sextic constants could not be satisfactorily determined. These values were held constant at their computed values. Based upon the satisfactory agreement between the computed and experimental spectroscopic constants, we believe that the spectroscopic constants provided in each least-squares fit are physically meaningful.

4.5. Search for the elusive axial isocyanocyclobutane

Unlike the cyano isomer, transitions for *axial* isocyanocyclobutane were not able to be assigned in the spectrum. They were not readily apparent as small bands moving across the equatorial spectrum like those seen for *axial* cyanocyclobutane (compare Figs. 3 and 7). The inability to assign *axial* isocyanocyclobutane may be due to several factors: lower abundance, as a consequence of the larger *axial* / *equatorial* energy difference for the isonitrile (1.4 kcal/mol) vs the nitrile

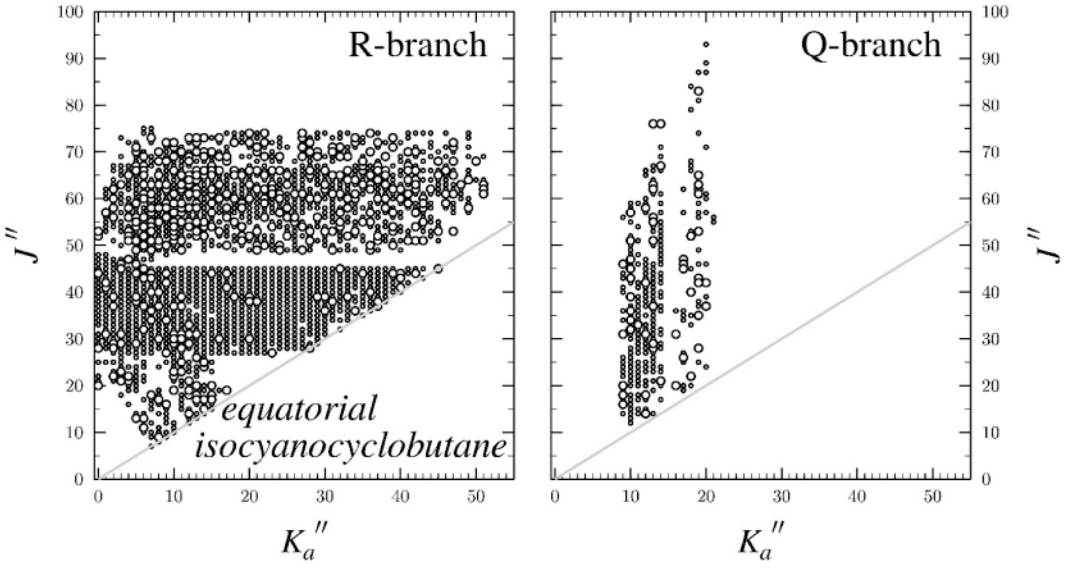

Fig. 6. Data distribution plots for the least-squares fit of spectroscopic data for the vibrational ground state of *equatorial* isocyanocyclobutane. The size of the symbol is proportional to the value of $|(f_{obs.} - f_{calc.})/\delta f|$, where δf is the frequency measurement uncertainty.

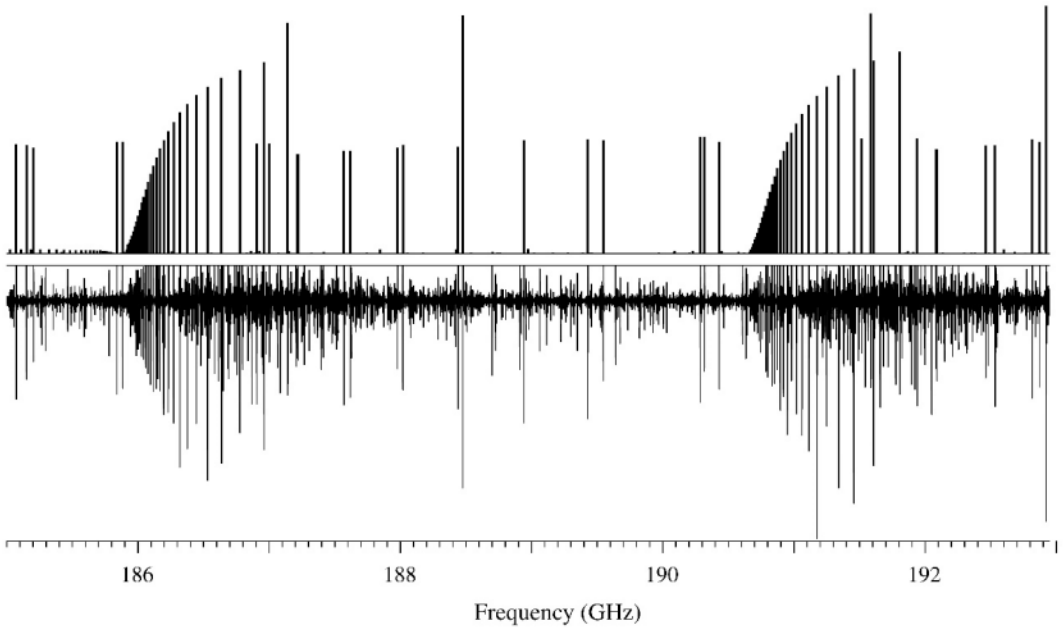

Fig. 7. Predicted (top) and experimental (bottom) rotational spectra of isocyanocyclobutane from 185 to 193 GHz. Ground-state *equatorial* isocyanocyclobutane transitions are shown for the $J' = 39$ and $J' = 40$ bands. Unassigned transitions are predominantly attributable to vibrationally excited states of *equatorial* isocyanocyclobutane.

Table 3
Spectroscopic constants for the ground vibrational state of *equatorial* isocyanocyclobutane (S- and A-reduced Hamiltonian, I^r representation).

	S Reduction, I^r representation			A Reduction, I^r representation	
	Experimental	B3LYP [a]		Experimental	B3LYP [a]
A_0 (MHz)	9823.21409 (36)	9686.7	A_0 (MHz)	9823.21373 (35)	9686.7
B_0 (MHz)	2542.019190 (63)	2525.6	B_0 (MHz)	2542.022183 (65)	2525.6
C_0 (MHz)	2226.550990 (71)	2208.5	C_0 (MHz)	2226.547590 (78)	2208.5
D_J (kHz)	0.366903 (17)	0.361	Δ_J (kHz)	0.383450 (21)	0.377
D_{JK} (kHz)	1.10893 (11)	0.965	Δ_{JK} (kHz)	1.00867 (12)	0.869
D_K (kHz)	13.3823 (16)	14.4	Δ_K (kHz)	13.4655 (16)	14.4
d_1 (kHz)	−0.016038 (14)	−0.0158	δ_J (kHz)	0.016059 (14)	0.0158
d_2 (kHz)	−0.0083226 (31)	−0.00796	δ_K (kHz)	1.57059 (57)	1.49
H_J (Hz)	0.0004756 (17)	0.000464	Φ_J (Hz)	0.0004816 (21)	0.000481
H_{JK} (Hz)	−0.004378 (16)	−0.00380	Φ_{JK} (Hz)	−0.001738 (30)	−0.000977
H_{KJ} (Hz)	0.055259 (91)	0.0492	Φ_{KJ} (Hz)	0.045768 (97)	0.0395
H_K (Hz)	−0.1540 (21)	−0.166	Φ_K (Hz)	−0.1483 (21)	−0.159
h_1 (Hz)	−0.0000342 (20)	−0.0000252	ϕ_J (Hz)	−0.0000272 (20)	−0.0000213
h_2 (Hz)	[0.00000833]	0.00000833	ϕ_{JK} (Hz)	[0.00141]	0.00141
h_3 (Hz)	[0.00000389]	0.00000389	ϕ_K (Hz)	[0.0831]	0.0831
L_J (mHz)	[0.]		L_J (μHz)	[0.]	
L_{JJK} (mHz)	[0.]		L_{JJK} (μHz)	0.0000246 (30)	
L_{JK} (mHz)	−0.0004526 (92)		L_{JK} (μHz)	−0.000554 (10)	
L_{KKJ} (mHz)	0.001076 (30)		L_{KKJ} (μHz)	0.001283 (30)	
L_K (mHz)	[0.]		L_K (μHz)	[0.]	
Δ_i (uÅ^2) [b,c]	−23.279075 (9)		Δ_i (uÅ^2) [b,c]	−23.278496 (10)	
P_{bb} (uÅ^2) [c,d]	39.807881 (3)		P_{bb} (uÅ^2) [c,d]	39.808173 (3)	
N_{lines} [e]	2296		N_{lines} [e]	2296	
σ_{fit} (MHz)	0.039		σ_{fit} (MHz)	0.039	

[a] Evaluated with the 6–311+G(2d,p) basis set. The computational output files label the representation as II^l, though we are confident that those constants are I^l which have been converted to I^r.
[b] Inertial defect, $\Delta_i = I_c - I_a - I_b$.
[c] Calculated using PLANM from the B_0 constants.
[d] Second moment, $P_{bb} = (I_c + I_a - I_b)/2$.
[e] Number of fitted transition frequencies.

(0.73 kcal/mol); additional spectral congestion arising from impurities in the synthesized sample, making the patterns less recognizable; or increased perturbation of transition frequencies due to coupling with the vibrationally excited states of the equatorial conformation, relative to the nitrile isomer. Attempts to predict the spectrum using the computed constants (B3LYP) or from empirical shifts derived from the experimental and computed constants of *axial* cyanocyclobutane were insufficient to identify this conformer by Loomis-Wood plots of its predicted series. While we are confident that the *axial* conformational isomer should have transitions with observable intensities in our frequency range, a successful detection appears to require higher sample purity of isocyanocyclobutane, better initial predictions, and/or addressing the

Coriolis coupling of this conformer to other vibrational states.

4.6. Ratio of axial and equatorial cyanocyclobutane

Utilizing transitions for the *equatorial* and *axial* conformers of cyanocyclobutane that have been confidently assigned and measured, it is possible to estimate the *equatorial* to *axial* ratio using the same methodology recently employed for determining the ratio of *anti*- to *gauche*-4-cyano-1-butyne [50]. This method, which relies on predicted intensities from SPCAT using the previously reported dipole moments for each conformer [26,27], yields an energy difference of 0.69 (7) kcal/mol for the *equatorial* and *axial* conformers of cyanocyclobutane. This value is consistent with the value reported by Caminati *et al.* of 0.73 (14) kcal/mol [27]. The newly determined value of 0.69 (7) kcal/mol is in good agreement with the computed value of 0.9 kcal/mol (B3LYP; Fig. 2). This close agreement for cyanocyclobutane gives us confidence that the conformational equilibrium of *axial* and *equatorial* isocyanocyclobutane is also being reasonably modeled *via* B3LYP. Using the computed energy difference of 1.4 kcal/mol, the *axial* to *equatorial* ratio for isocyanocyclobutane should be approximately 0.09 at 298 K. Details of the analysis are provided in the supplementary material.

4.7. Structural interpretation of the rotational constants

For the set of non-planar, C_s symmetry molecules presented in this work, a few conclusions are possible concerning these structures by analyzing the Δ_i and P_{bb} constants provided in Tables 1, 2, and 3 [51]. The inertial defect values (Δ_i) provide structural information regarding the extent to which all of the atoms are not located on the *ab* plane. The similarity between the inertial defects of *equatorial* cyano- and isocyanocyclobutane (differing by less than 2 %) is not surprising given their structural similarity. As is shown in Fig. 2., the *ab* plane lies just below the carbon atom bonded to the CN group and nearly bisects the CN substituent. In contrast, when the CN group is *axial*, the principal axes rotate to place the ring atoms and CN group further from the *ab* plane, nearly causing a doubling of the inertial defect. The second moment P_{bb} is arguably a more meaningful structural parameter. Due to the C_s nature of these species, where the plane of symmetry coincides with the *ac* plane, P_{bb} provides direct information about the distance of the CH_2 groups relative to the *ac* plane. For *axial* and *equatorial* cyanocyclobutane the S-reduction value of P_{bb} is remarkably consistent (39.902 and 39.900, respectively), indicating that the ring-puckering is not substantially impacted by the orientation of the cyano group. There are only slight differences in the P_{bb} values of mono-substituted cyclobutanes shown in Table 4, which indicates that the structure of the cyclobutane rings are reasonably consistent regardless of substitution of σ electron-withdrawing substituents with low steric profile. This is expected given the aforementioned consistency of the potential energy surfaces of these species.

5. Conclusion

The transition frequencies and spectroscopic constants for cyanocyclobutane and isocyanocyclobutane, presented in this work, provide the foundation for future astronomical searches for these molecules. Combined with nuclear hyperfine coupling constants, these constants should be useful for predicting lower or slightly higher energy transition frequencies reliably. Nuclear hyperfine coupling constants for isocyanocyclobutane need to be measured or estimated from high level *ab initio* calculations to enable this analysis. Our study also revealed previously unrecognized Coriolis-coupling interactions between the *axial* conformation of cyanocyclobutane and the vibrationally excited states of the *equatorial* conformation. In order to implement the challenging analysis of these couplings, additional spectroscopy including high resolution infrared spectroscopy would be very beneficial, due to the potentially large number of involved vibrational states and their close energy spacing.

Table 4
Second Moments (P_{bb}) for Mono-substituted Cyclobutanes.

Species	P_{bb} (uÅ^2)	Reference
fluorocyclobutane (*ax*)	39.967	[52]
fluorocyclobutane (*eq*)	39.805	[52]
chlorocyclobutane (*ax*)[a]	39.830	[53]
chlorocyclobutane (*eq*)[a]	39.842	[53]
bromocyclobutane (*eq*)[a]	39.943	[54]
cyanocyclobutane (*ax*)	39.902	this work
cyanocyclobutane (*eq*)	39.900	this work
isocyanocyclobutane (eq)	39.808	this work

[a] Data provided for the most abundant isotopologue.

6. Synthetic procedures and characterization

***N*-Cyclobutylformamide** [37,44]. In a single-neck 100 mL round-bottom flask, 6.12 g (86 mmol) cyclobutylamine and 60 mL (742 mmol) ethyl formate were combined. The reaction flask was connected to a water-cooled reflux condenser, and the stirred reaction was heated to reflux for 4 hr. After cooling to room temperature, excess ethyl formate was removed *in vacuo* to yield the crude product as a yellow oil. The crude oil was purified *via* short-path vacuum distillation (bp = 72 °C, 1 Torr) to yield *N*-cyclobutylformamide as a viscous, colorless oil (8.29 g, 97 %). ^{1}H NMR ($CDCl_3$, 400 MHz): The product was observed as two separate conformational isomers in a 4:1 ratio. δ (ppm) ***equatorial*:** 8.03 (s, 1H), 7.30 (brs, 1H), 4.43 (m, 1H), 2.31 (m, 2H) 1.97 (m, 2H), 1.72 (m, 2H). ***axial*:** 8.06 (s, 1H), 7.20 (brs, 1H), 4.00 (m, 1H), 2.31 (m, 2H) 1.97 (m, 2H), 1.72 (m, 2H). ^{13}C NMR ($CDCl_3$, 100 MHz): δ (ppm) ***equatorial*:** 160.6, 43.3, 30.7, 15.1. ***axial*:** 163.5, 47.3, 31.6, 14.4. IR (neat): (cm^{-1}) 3269 (m), 3047 (w), 2978 (m), 2862 (m), 1652 (s), 1528 (m), 1384 (m), 1344 (m), 1303 (m), 1253 (m), 730 (m), 600 (w), 455 (m). HRMS: $[M + H]^+$ Calculated for $C_5H_{10}NO$: 100.0757. Found: 100.0755; $[M + Na]^+$ Calculated for C_5H_9NONa: 122.0576. Found: 122.0574.

Isocyanocyclobutane [37]. In a flame-dried, single-neck 100 mL round-bottom flask (cooled under a stream of N_2), 24.23 g (127 mmol) *p*-toluenesulfonyl chloride and 49 g (380 mmol) dry quinoline were combined. The flask was then connected to a one-piece Claisen-type distillation apparatus with a 50 mL receiving vessel. The Claisen head was sealed with a rubber septum and the system was purged (2 ×) *via* vacuum/N_2 backfill cycles. The receiving vessel was cooled with liquid nitrogen and the boiling flask was heated to 50 °C in an oil bath. *N*-Cyclobutylformamide (8.29 g, 83.7 mmol) was then added dropwise to the heated solution of *p*-toluenesulfonyl chloride/quinoline over a course of 10 min *via* syringe needle. A vacuum (100 Torr) was applied to the system, and the crude distillate was collected over the next 40 min. The resulting distillate was further purified (to remove traces of quinoline) *via* trap-to-trap distillation (2 ×) to yield isocyanocyclobutane (2.71 g, 40 %) as a volatile, colorless oil with an intense, foul odor. ^{1}H NMR ($CDCl_3$, 500 MHz): δ (ppm) 3.95 (*p*, 1H, *J* = 8 Hz), 2.42 (*m*, 2H), 2.32 (*m*, 2H), 1.90 (*m*, 1H) 1.79 (*m*, 1H). ^{13}C NMR ($CDCl_3$, 125 MHz): δ (ppm) 155.3, 45.0, 31.1, 15.9. IR (neat): (cm^{-1}) 2994 (m), 2955 (m), 2874 (w), 2137 (s), 1444 (w), 1347 (m), 1248 (w), 1123 (w), 1052 (m), 937 (m), 896 (m), 746 (w), 467 (m). HRMS: $[M + H]^+$ Calculated for C_5H_8N: 82.0651. Found: 82.0648.

Declaration of Competing Interest

The authors declare that they have no known competing financial interests or personal relationships that could have appeared to influence the work reported in this paper.

Data availability

Data will be made available on request.

Acknowledgments

We gratefully acknowledge the National Science Foundation for support of this project (CHE-1954270). We thank Michael McCarthy for the loan of an amplification-multiplication chain. We thank the following organizations and individuals for support of shared departmental facilities: Bruker AVANCE 400 NMR spectrometer (NSF CHE-1048642), Bruker AVANCE 500 NMR spectrometer (gift from Paul J. and Margaret M. Bender), and Thermo Scientific Q Exactive Plus mass spectrometer (NIH 1S10 OD020022-1). We thank Maria Zdanovskaia for her assistance with generating figures.

Appendix A. Supplementary material

Computational chemistry output files, least-squares fitting output files from SPFIT, and experimental IR, ^{1}H NMR, ^{13}C NMR, and mass spectra of all synthesized compounds.

Supplementary data to this article can be found online at https://doi.org/10.1016/j.jms.2022.111684.

References

[1] H.S.P. Müller, F. Schlöder, J. Stutzki, G. Winnewisser, The Cologne Database for Molecular Spectroscopy, CDMS: a Useful Tool for Astronomers and Spectroscopists, J. Mol. Struct. 742 (1–3) (2005) 215–227.
[2] H.S.P. Müller, S. Thorwirth, D.A. Roth, G. Winnewisser, The Cologne Database for Molecular Spectroscopy, CDMS, Astron. Astrophys. 370 (3) (2001) L49–L52.
[3] L.E. Snyder, D. Buhl, Detection of Several New Interstellar Molecules, Ann. New York Acad. Sci. 194 (1 Interstellar) (1972) 17–24.
[4] B. Zuckerman, M. Morris, P. Palmer, B.E. Turner, Observations of CS, HCN, U89.2, and U90.7 in NGC 2264, Astrophys. J. 173 (1972) L125–L129.
[5] J. Cernicharo, C. Kahane, M. Guelin, J. Gomez-Gonzalez, Tentative Detection of CH_3NC towards SGR B2, Astron. Astrophys. 189 (1988) L1–L2.
[6] P.M. Solomon, K.B. Jefferts, A.A. Penzias, R.W. Wilson, Detection of Millimeter Emission Lines from Interstellar Methyl Cyanide, Astrophys. J. 168 (1971) L107–L110.
[7] K. Kawaguchi, M. Ohishi, S.-I. Ishikawa, N. Kaifu, Detection of Isocyanoacetylene HCCNC in TMC-1, Astrophys. J. 386 (1992) L51–L53.
[8] N.W. Broten, J.M. MacLeod, L.W. Avery, W.M. Irvine, B. Hoglund, P. Friberg, A. Hjalmarson, The detection of interstellar methylcyanoacetylene, Astrophys. J. 276 (1984) L25–L29.
[9] N.W. Broten, T. Oka, L.W. Avery, J.M. MacLeod, H.W. Kroto, The detection of HC_9N in interstellar space, Astrophys. J. 223 (1978) L105–L107.
[10] F.F. Gardner, G. Winnewisser, The detection of interstellar vinyl cyanide (acrylonitrile), Astrophys. J. 195 (1975) L127–L130.
[11] F.J. Lovas, A.J. Remijan, J.M. Hollis, P.R. Jewell, L.E. Snyder, Hyperfine Structure Identification of Interstellar Cyanoallene toward TMC-1, Astrophys. J. 637 (1) (2006) L37–L40.
[12] C.N. Shingledecker, K.L.K. Lee, J.T. Wandishin, N. Balucani, A.M. Burkhardt, S. B. Charnley, R. Loomis, M. Schreffler, M. Siebert, M.C. McCarthy, B.A. McGuire, Detection of interstellar H_2CCCHC_3N, Astron. Astrophys. 652 (2021) L12.
[13] M.A. Siebert, K.L.K. Lee, A.J. Remijan, A.M. Burkhardt, R.A. Loomis, M. C. McCarthy, B.A. McGuire, CH_3-Terminated Carbon Chains in the GOTHAM Survey of TMC-1: Evidence of Interstellar CH_3C_7N, Astrophys. J. 924 (1) (2022) 21.
[14] L.E. Snyder, T.L. Wilson, C. Henkel, P.R. Jewell, C.M. Walmsley, Detection of Interstellar Methylcyanodiacetylene in the Dark Dust Cloud TMC 1, Bull. Am. Astron. Soc. 16 (1984) 959.
[15] B.A. McGuire, R.A. Loomis, A.M. Burkhardt, K.L.K. Lee, C.N. Shingledecker, S. B. Charnley, I.R. Cooke, M.A. Cordiner, E. Herbst, S. Kalenskii, M.A. Siebert, E. R. Willis, C.i. Xue, A.J. Remijan, M.C. McCarthy, Detection of two interstellar polycyclic aromatic hydrocarbons via spectral matched filtering, Science 371 (6535) (2021) 1265–1269.
[16] B.A. McGuire, A.M. Burkhardt, S. Kalenskii, C.N. Shingledecker, A.J. Remijan, E. Herbst, M.C. McCarthy, Detection of the aromatic molecule benzonitrile (c-C_6H_5CN) in the interstellar medium, Science 359 (6372) (2018) 202–205.
[17] K.L. Kelvin Lee, P.B. Changala, R.A. Loomis, A.M. Burkhardt, C.i. Xue, M. A. Cordiner, S.B. Charnley, M.C. McCarthy, B.A. McGuire, Interstellar Detection of 2-cyanocyclopentadiene, C_5H_5CN, a Second Five-membered Ring toward TMC-1, Astrophys. J. 910 (1) (2021) L2.
[18] M.C. McCarthy, K.L.K. Lee, R.A. Loomis, A.M. Burkhardt, C.N. Shingledecker, S. B. Charnley, M.A. Cordiner, E. Herbst, S. Kalenskii, E.R. Willis, C.i. Xue, A. J. Remijan, B.A. McGuire, Interstellar detection of the highly polar five-membered ring cyanocyclopentadiene, Nat. Astron. 5 (2) (2021) 176–180.
[19] A. Belloche, R.T. Garrod, H.S.P. Müller, K.M. Menten, C. Comito, P. Schilke, Increased complexity in interstellar chemistry: detection and chemical modeling of ethyl formate and *n*-propyl cyanide in Sagittarius B2(N), Astron. Astrophys. 499 (1) (2009) 215–232.
[20] A. Belloche, T. Garrod Robin, S.P. Müller Holger, M. Menten Karl, Detection of a branched alkyl molecule in the interstellar medium: *iso*-propyl cyanide, Science 345 (6204) (2014) 1584–1587.
[21] H.H. Smith, S.M. Kougias, B.J. Esselman, R.C. Woods, R.J. McMahon, Synthesis, Purification, and Rotational Spectroscopy of 1-Cyanocyclobutene (C_5H_5N), J. Phys. Chem. A 126 (12) (2022) 1980–1993.
[22] D.L. Powell, A. Gatial, P. Klaeboe, C.J. Nielsen, A.J. Kondow, W.A. Boettner, A. M. Mulichak, Vibrational spectra and conformations of cyanocyclobutane, Acta Chem. Scand. 43 (5) (1989) 441–449.
[23] F. Vazart, C. Latouche, P. Cimino, V. Barone, Accurate Infrared (IR) Spectra for Molecules Containing the C≡N Moiety by Anharmonic Computations with the Double Hybrid B2PLYP Density Functional, J. Chem. Theor. Comput. 11 (9) (2015) 4364–4369.
[24] J.R. Durig, A. Ganguly, J.J. Klaassen, G.A. Guirgis, The r_0 structural parameters, conformational stability, and vibrational assignment of *equatorial* and *axial* cyanocyclobutane, J. Mol. Struct. 923 (1) (2009) 28–38.
[25] M.Y. Fong, M.D. Harmony, Microwave spectrum, dipole moment, quadrupole coupling constants, and conformation of cyanocyclobutane, J. Chem. Phys. 58 (10) (1973) 4260–4264.
[26] J.R. Durig, L.A. Carreira, W.J. Lafferty, Spectra and structure of small ring compounds. Microwave spectrum of cyanocyclobutane, J. Mol. Spectrosc. 46 (2) (1973) 187–193.
[27] W. Caminati, B. Velino, M. Dakkouri, L. Schäfer, K. Siam, J.D. Ewbank, Reinvestigation of the microwave spectrum of cyanocyclobutane: Assignment of the *axial* conformer, J. Mol. Spectrosc. 123 (2) (1987) 469–475.
[28] M. Dakkouri, H. Ephardt, K. Siam, L. Schäfer, C. Van Alsenoy, A combined ab initio and gas electron diffraction study of the molecular structure of 1,1-dicyanocyclobutane, J. Mol. Struct. 159 (1) (1987) 123–135.
[29] W. Caminati, B. Velino, R.G. Della Valle, Rotational spectra of several vibrational excited states of *axial* and *equatorial* cyanocyclobutane and potential energy function of the ring puckering, J. Mol. Spectrosc. 129 (2) (1988) 284–292.
[30] T. Egawa, T. Fukuyama, S. Yamamoto, F. Takabayashi, H. Kambara, T. Ueda, K. Kuchitsu, Molecular structure and puckering potential function of cyclobutane studied by gas electron diffraction and infrared spectroscopy, J. Chem. Phys. 86 (11) (1987) 6018–6026.
[31] D.L. Powell, A. Gatial, P. Klaeboe, C.J. Nielsen, A.J. Kondow, Conformational behaviour of five cyclobutane derivatives, J. Mol. Struct. 173 (1988) 389–396.
[32] R. Pasternak, A.Y. Meyer, Cyclobutane: a unified theoretical approach, J. Mol. Struct. 13 (2) (1972) 201–210.
[33] A. Gatial, P. Klaeboe, C.J. Nielsen, D.L. Powell, D. Sülzle, A.J. Kondow, Vibrational spectra and conformations of chloro- and bromo-cyclobutane, J. Raman Spectrosc. 20 (4) (1989) 239–250.
[34] M. Meier, B. Dogan, D. Beckhaus, C. Ruechardt, Heats of formation and heats of isomerization of isocyanides, New J. Chem. 11 (1) (1987) 1–6.
[35] M. Meier, B. Mueller, C. Ruechardt, The isonitrile-nitrile rearrangement. A reaction without a structure-reactivity relationship, J. Org. Chem. 52 (4) (1987) 648–652.
[36] W. Dianxun, Q. Ximei, Z. Qiyuan, The isonitrile-nitrile isomerization: kinetic parameters, reaction mechanism and relative photoionization cross-section of the HOMO. A HeI photoelectron spectroscopy study, Chem. Phys. Lett. 266 (5) (1997) 560–567.
[37] J. Casanova Jr., R.E. Schuster, N.D. Werner, Synthesis of aliphatic isocyanides, J. Chem. Soc. (Aug.) (1963) 4280–4281.
[38] J. Casanova, N.D. Werner, R.E. Schuster, The Isonitrile—Nitrile Isomerization, J. Org. Chem. 31 (11) (1966) 3473–3482.
[39] **Z. Li, X. Xu, Y. Chen, J. Liu, W. Li, Preparation of 6-substituted benzodiazepine-2,4-dione compounds for treating cancer, East China University of Science and Technology, Peop. Rep. China; Chinese patent, CN 103435562 (Dec 11, 2013).**
[40] **M.J. Orwat, D.J.P. Pinto, L.M. Smith, II, S. Srivastava, Preparation of substituted tetrahydroisoquinoline compounds as factor Xia inhibitors, Bristol-Myers Squibb Company, USA; WO patent, WO 2013056034 (Apr 18, 2013).**
[41] P. Capurro, L. Moni, A. Galatini, C. Mang, A. Basso, Multi-Gram Synthesis of Enantiopure 1,5-Disubstituted Tetrazoles Via Ugi-Azide 3-Component Reaction, Molecules 23 (11) (2018) 2758.
[42] **M.J. Frisch, G.W. Trucks, H.B. Schlegel, G.E. Scuseria, M.A. Robb, J.R. Cheeseman, G. Scalmani, V. Barone, G.A. Petersson, H. Nakatsuji, X. Li, M. Caricato, A.V. Marenich, J. Bloino, B.G. Janesko, R. Gomperts, B. Mennucci, H.P. Hratchian, J.V. Ortiz, A.F. Izmaylov, J.L. Sonnenberg, D. Williams-Young, F. Ding, F. Lipparini, F. Egidi, J. Goings, B. Peng, A. Petrone, T. Henderson, D. Ranasinghe, V.G. Zakrzewski, J. Gao, N. Rega, G. Zheng, W. Liang, M. Hada, M. Ehara, K. Toyota, R. Fukuda, J. Hasegawa, M. Ishida, T. Nakajima, Y. Honda, O. Kitao, H. Nakai, T. Vreven, K. Throssell, J.A. Montgomery, Jr. , J.E. Peralta, F. Ogliaro, M.J. Bearpark, J.J. Heyd, E.N. Brothers, K.N. Kudin, V.N. Staroverov, T.A. Keith, R. Kobayashi, J. Normand, K. Raghavachari, A.P. Rendell, J.C. Burant, S.S. Iyengar, J. Tomasi, M. Cossi, J.M. Millam, M. Klene, C. Adamo, R. Cammi, J.W. Ochterski, R.L. Martin, K. Morokuma, O. Farkas, J.B. Foresman, D.J. Fox, Gaussian 16 rev C.01, Gaussian, Inc., Wallingford, CT, USA, 2016.**
[43] **J.R. Schmidt, W.F. Polik, WebMO Enterprise, version 19.0; WebMO LLC: Madison, WI, USA, 2019; http://www.webmo.net (accessed August, 2019).**
[44] G. Giardina, G.D. Clarke, G. Dondio, G. Petrone, M. Sbacchi, V. Vecchietti, Selective.kappa.-Opioid Agonists: Synthesis and Structure-Activity Relationships of Piperidines Incorporating an Oxo-Containing Acyl Group, J. Med. Chem. 37 (21) (1994) 3482–3491.

[45] B.K. Amberger, B.J. Esselman, J.F. Stanton, R.C. Woods, R.J. McMahon, Precise Equilibrium Structure Determination of Hydrazoic Acid (HN_3) by Millimeter-wave Spectroscopy, J. Chem. Phys. 143 (10) (2015), 104310.
[46] B.J. Esselman, B.K. Amberger, J.D. Shutter, M.A. Daane, J.F. Stanton, R.C. Woods, R.J. McMahon, Rotational spectroscopy of pyridazine and its isotopologs from 235–360 GHz: Equilibrium structure and vibrational satellites, J. Chem. Phys. 139 (22) (2013), 224304.
[47] Z. Kisiel, L. Pszczółkowski, B.J. Drouin, C.S. Brauer, S. Yu, J.C. Pearson, I. R. Medvedev, S. Fortman, C. Neese, Broadband rotational spectroscopy of acrylonitrile: Vibrational energies from perturbations, J. Mol. Spectrosc. 280 (2012) 134–144.
[48] Z. Kisiel, L. Pszczółkowski, I.R. Medvedev, M. Winnewisser, F.C. De Lucia, E. Herbst, Rotational spectrum of *trans–trans* diethyl ether in the ground and three excited vibrational states, J. Mol. Spectrosc. 233 (2) (2005) 231–243.
[49] H.M. Pickett, The fitting and prediction of vibration-rotation spectra with spin interactions, J. Mol. Spectrosc. 148 (2) (1991) 371–377.
[50] P.M. Dorman, B.J. Esselman, P.B. Changala, S.M. Kougias, M.C. McCarthy, R. C. Woods, R.J. McMahon, Rotational spectrum of *anti*- and *gauche*-4-cyano-1-butyne (C_5H_5N) – An open-chain isomer of pyridine, J. Mol. Spectrosc. 385 (2022), 111604.
[51] R.K. Bohn, J.A. Montgomery, H.H. Michels, J.A. Fournier, Second moments and rotational spectroscopy, J. Mol. Spectrosc. 325 (2016) 42–49.
[52] W. Caminati, L.B. Favero, A. Maris, P.G. Favero, Microwave spectrum of the *axial* conformer and potential energy function of the ring puckering motion in fluorocyclobutane, J. Mol. Struct. 376 (1) (1996) 25–32.
[53] B. Velino, L.B. Favero, W. Caminati, Rotational Spectrum of the *Axial* Form and Conformational Equilibrium in Chlorocyclobutane, J. Mol. Spectrosc. 179 (1) (1996) 168–174.
[54] W.G. Rothschild, B.P. Dailey, Microwave Spectrum of Bromocyclobutane, J. Chem. Phys. 36 (11) (1962) 2931–2940.